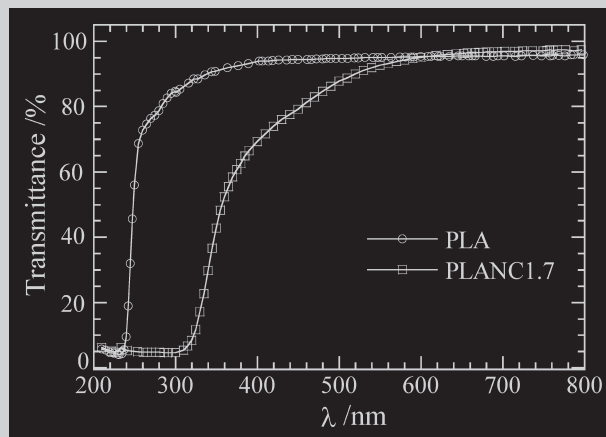


**Summary:** The preparation and characterization of a new type of nanocomposite material that is based on biodegradable polylactide (PLA) and organically modified layered titanate, is reported. Layered titanate, modified with a *N*-(cocoalkyl)-*N,N*-[bis(2-hydroxyethyl)]-*N*-methylammonium cation, was used as a new nanofiller (OHTO) for the nanocomposite preparation. Wide-angle X-ray diffraction and transmission electron microscopy (TEM) analyses confirmed that titanate layers were intercalated and nicely distributed in the PLA matrix. The materials properties of neat PLA improved remarkably after nanocomposite preparation.

UV/vis transmission spectra of neat PLA and a nanocomposite.



# Organically Modified Layered Titanate: A New Nanofiller to Improve the Performance of Biodegradable Polylactide

Ryoichi Hiroi,<sup>2</sup> Suprakas Sinha Ray,<sup>1</sup> Masami Okamoto,\*<sup>1</sup> Takashi Shiroy<sup>2</sup>

<sup>1</sup>Toyota Technological Institute, Advanced Polymeric Materials Engineering, Graduate School of Engineering, Toyota Technological Institute, Hisakata 2-12-1, Tempaku, Nagoya 468-8511, Japan

Fax: (+81) 52 809 1864; E-mail: okamoto@toyota-ti.ac.jp

<sup>2</sup>Otsuka Chemicals Co. Ltd, Advanced Material Products Group, Research & Technical Center, Otsuka Chemicals Co. Ltd., Kagasuno Kawauchi-Cho 463, Tokushima 771-0193, Japan

Received: April 30, 2004; Revised: June 1, 2004; Accepted: June 1, 2004; DOI: 10.1002/marc.200400173

**Keywords:** biodegradable; degradation; layered titanate; nanocomposites; polylactides

## Introduction

Over the last few years, the utility of inorganic nanoscale particles as filler to enhance polymer performance has been established. Of particular interest is recently developed nanocomposite technology consisting of a polymer and organically modified layered silicate (OMLS) because they often exhibit remarkably improved mechanical and various other materials properties as compared with those of the virgin polymer.<sup>[1]</sup>

In our recent publications,<sup>[2,3]</sup> we have reported the preparation, characterization, mechanical and various other properties, crystallization behavior, biodegradability, melt rheology, and finally foam processing of a series of polylactide (PLA)/OMLS nanocomposites.

In this communication, and for the first time, we report the preparation and characterization of a new type of

biodegradable nanocomposite material that is based on biodegradable PLA and organically modified layered titanate, as a new nanofiller.

## Experimental Part

### Materials

PLA with a *D*-isomer content of 1.1–1.7% ( $T_g = 60^\circ\text{C}$  and  $T_m = 168.0^\circ\text{C}$ ) was supplied by Unitika Co. Ltd., Japan, and was dried under vacuum at  $60^\circ\text{C}$ , and then kept under dry nitrogen gas for one week prior to use.

### Preparation of the Mixed Potassium Metal Complex<sup>[4]</sup>

A blend of  $\text{K}_2\text{CO}_3$  (304 g),  $\text{Li}_2\text{CO}_3$  (54 g),  $\text{TiO}_2$  (762 g), and  $\text{KCl}$  (136 g) was mixed intimately and heated at  $1020^\circ\text{C}$  for 4 h

in an electric furnace. After cooling, the powder was dispersed to a 5 wt.-% water slurry and 10 wt.-% of  $\text{H}_2\text{SO}_4$  water solution was added while agitating for 2 h until a pH of 7.0 was reached. The above slurry was filtered off and rinsed with water, and then dried at 110 °C. After this, it was heated at 600 °C for more than 3 h in an electric furnace. The obtained white powder was  $\text{K}_{0.7}\text{Ti}_{1.73}\text{Li}_{0.27}\text{O}_{3.95}$  with an average particle size of 32  $\mu\text{m}$ .

#### Protonation of the Layered Titanate (HTO)

$\text{K}_{0.7}\text{Ti}_{1.73}\text{Li}_{0.27}\text{O}_{3.95}$  (130 g) was stirred in 0.5 N HCl solution for 1.5 h at ambient temperature. After stirring, the product HTO was collected by filtration and washed with water. The obtained HTO was ion-exchanged, 72% of potassium ion and 99% or more lithium ion to proton. The powder X-ray diffraction pattern of the pristine HTO ( $\text{K}_{0.2}\text{H}_{0.77}\text{Ti}_{1.73}\text{O}_{3.95} \cdot 0.5 \text{H}_2\text{O}$ ) is shown in Figure 1. The chemical composition was determined by X-ray fluorescence analysis.

#### Preparation of Organically Modified Layered Titanate (OHTO)

The recovered HTO and *N*-(cocoalkyl)-*N,N*-[bis(2-hydroxyethyl)]-*N*-methylammonium chloride (157.5 g) were stirred at 80 °C for 1 h in doubly distilled water. After 1 h, the product was filtered and washed at 80 °C with water. The obtained organo-HTO was first dried at 40 °C for 1 d under air to prevent particle aggregation, and then at 160 °C for 12 h under vacuum.

#### Nanocomposite Preparation

For nanocomposite preparation, the organo-HTO (OHTO) (dried at 120 °C for 8 h) and PLA were first dry mixed by shaking them in a bag. The mixture was then melt-extruded using a twin-screw extruder (KZW15-30TGN, Technovel Corp.) operated at 195 °C (screw speed = 300 rpm, feed rate = 22  $\text{g} \cdot \text{min}^{-1}$ ) to yield nanocomposite strands. Hereafter, nanocomposites are abbreviated as PLANCs.

PLANCs prepared with two different amounts of inorganic titanate, that is, 1.7 and 3.9 wt.-%, are correspondingly abbreviated as PLANC1.7 and PLANC3.9, respectively.

The strands were pelletized and dried under vacuum at 70 °C for 7 h to remove water. The dried PLANCs pellets were then converted into sheets with a thickness of 0.7–2 mm by pressing with  $\sim 1.5$  MPa at 190 °C for 3 min. The molded sheets were then quickly quenched between glass plates and then annealed at 110 °C for 1.5 h to crystallize isothermally before being subjected to various characterizations.

#### Characterization Methods

Wide-angle X-ray Diffraction (WAXD) analyses were performed for the various OMLS powders and corresponding nanocomposite sheets using an MXlabo X-ray diffractometer (MAC Science Co., generator of 3 kW, a graphite monochromator, Cu  $\text{K}\alpha$  radiation (wavelength,  $\lambda = 0.154$  nm), operated at 40 kV/20 mA). The samples were scanned in fixed time (FT) mode with a counting time of 2 s under diffraction angle  $2\theta$  in the range of 1 to 70°.

The nanostructure of various nanocomposites was investigated by means of high-resolution transmission electron microscopy (TEM) (H-7100, Hitachi Co.) operated at an accelerating voltage of 100 kV. Ultra-thin sections of either crystallized pellets or sheets (perpendicular to the compression mold) with a thickness of  $\sim 100$  nm were microtomed at  $-80$  °C using a Reichert Ultra cut cryo-ultramicrotome without staining.

Weight-average ( $\bar{M}_w$ ) and number-average ( $\bar{M}_n$ ) molecular weights of PLA (before and after nanocomposites preparation) were determined by means of gel permeation chromatography (GPC) (LC-VP, Shimadzu Co.), using polystyrene standards for calibration and tetrahydrofuran (THF) as the carrier solvent at 40 °C with a flow rate of 0.5  $\text{mL} \cdot \text{min}^{-1}$ . For the GPC measurements, the PLA or nanocomposites were first dissolved in  $\text{CHCl}_3$  and then diluted with THF. GPC results of PLA and the two different nanocomposites are presented in Table 1. As anticipated, the incorporation of various kinds of OHTO resulted in a reduction in the molecular weight of the PLA matrix. Decreased molecular weights of nanocomposites may be explained by either the shear mixing of PLA and OHTO or the presence of hydroxy groups in the alkylammonium cation, both resulting in a certain degree of hydrolysis of the PLA matrix at high temperature.

The glass transition ( $T_g$ ), melting ( $T_m$ ), and crystallization ( $T_c$ ) temperatures, as well as the degree of crystallinity ( $\chi_c$ ) of pure PLA and the nanocomposites were determined by a temperature-modulated DSC (TMDSC) (MDSC<sup>TM</sup>, TA2920, TA instruments). The DSC was performed at a heating rate of 5 °C  $\cdot \text{min}^{-1}$  with a heating/cooling cycle of a modulation period of 60 s, and an amplitude of  $\pm 0.769$  °C. For the measurement of  $\chi_c$  prior to DSC analysis, the extra heat absorbed by the crystallites formed during heating had to be subtracted from the total endothermic heat flow because of melting of the whole crystallites. This can be done according to the principles and procedures described in our previous paper.<sup>[3]</sup> By considering the melting enthalpy of 100% crystalline poly(L-lactide) as 93  $\text{J} \cdot \text{g}^{-1}$ , we have estimated the value of the  $\chi_c$  of pure PLA and the nanocomposites, which are also presented in Table 1.

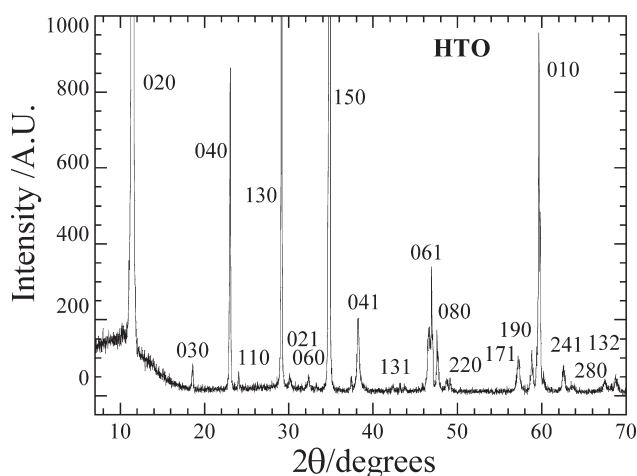


Figure 1. WAXD patterns of HTO powder.

Table 1. Characteristic parameters of neat PLA and the nanocomposites.

Samples	$\bar{M}_w \times 10^{-3}$ g · mol <sup>-1</sup>	$\bar{M}_w/\bar{M}_n$	$T_g$ °C	$T_m$ °C	$T_c$ °C	$\chi_c$ %
PLA	210	1.46	60	168	127.2	36
PLANC1.7	138	1.75	58	166.5	96.2	41.8
PLANC3.9	113	1.72	57	165.6	94.1	43.2

The dried neat PLA and PLANCs pellets were injection molded using an injection machine (IS-80G, Toshiba Machinery Co.) operated at 190 °C with a mold temperature of 30 °C. Flexural modulus and strength of the injection-molded specimens (thickness ~3.2 mm, annealed at 120 °C for 30 min) were measured according to an ASTM D-790 method with a strain rate of 2 mm · min<sup>-1</sup> at room temperature.

Ultraviolet (UV)/visible (vis) transmission behavior was measured by a UV/vis spectrophotometer (U-3000, Hitachi Co.), operated with a scanning rate of 5 nm · s<sup>-1</sup> under reflection mode. Photodegradability (sunshine weathering) of neat PLA and the nanocomposites was studied on a sunshine weathermeter (WEL-SUN-DC, Suga Test instruments) operated at 60 °C.

## Results and Discussion

WAXD patterns for the pure OHTO powder and two nanocomposites (PLANCs) are presented in Figure 2. The mean interlayer spacing of the (001) plane ( $d_{(001)}$ ) for the OHTO solid obtained by WAXD measurements is 2.26 nm ( $2\theta \cong 3.90^\circ$ ). The appearance of a small peak observed at  $2\theta \cong 7.70^\circ$  confirmed that this reflection is caused by a (002) plane ( $d_{(002)}$ ) of OHTO. In the case of PLANC1.7, a very small peak is observed at  $2\theta \cong 3.69^\circ$  ( $\cong 2.40$  nm), corresponding to the (001) plane of the dispersed titanate layers in the PLA matrix. With increasing OHTO content, this peak becomes stronger without significant peak shift for PLANC3.9, accompanied with the appearance of a small peak. After calculation, it was confirmed that this reflection is because of the (002) plane of OHTO dispersed in the PLA matrix. The difference in interlayer spacing between pure OHTO powder and PLANC1.7 to PLANC3.9 after melt mixing is presumably because of intercalation of PLA chains into the titanate galleries, and the coherent order of the titanate layers is much higher with increasing OHTO content. Note that the existence of a sharp Bragg peak in PLANCs after melt extrusion clearly indicates that the dispersed titanate layers still retain an ordered structure after melt extrusion.

From WAXD patterns, the crystallite size of intercalated stacked titanate layers of each PLANC is calculated by using Scherrer equation, that is,  $D$  is given by Equation (1).<sup>5,6]</sup>

$$D = \frac{k \cdot \lambda}{\beta \cdot \cos \theta} \quad (1)$$

$k$  is a constant (the value generally = 0.9),  $\lambda$  is the X-ray

wavelength (=0.154 nm),  $\beta$  is the width of the WAXD peak (in radian units) and is measured by the full width at half maximum, and  $\theta$  is the WAXD peak position. The calculated value of  $D$  for each PLANC is presented in Table 2.

The internal structure of the nanocomposites on the nanometer scale was directly observed by TEM analyses. Figure 3 shows the results of TEM bright-field images of PLANCs corresponding to the WAXD experiments as

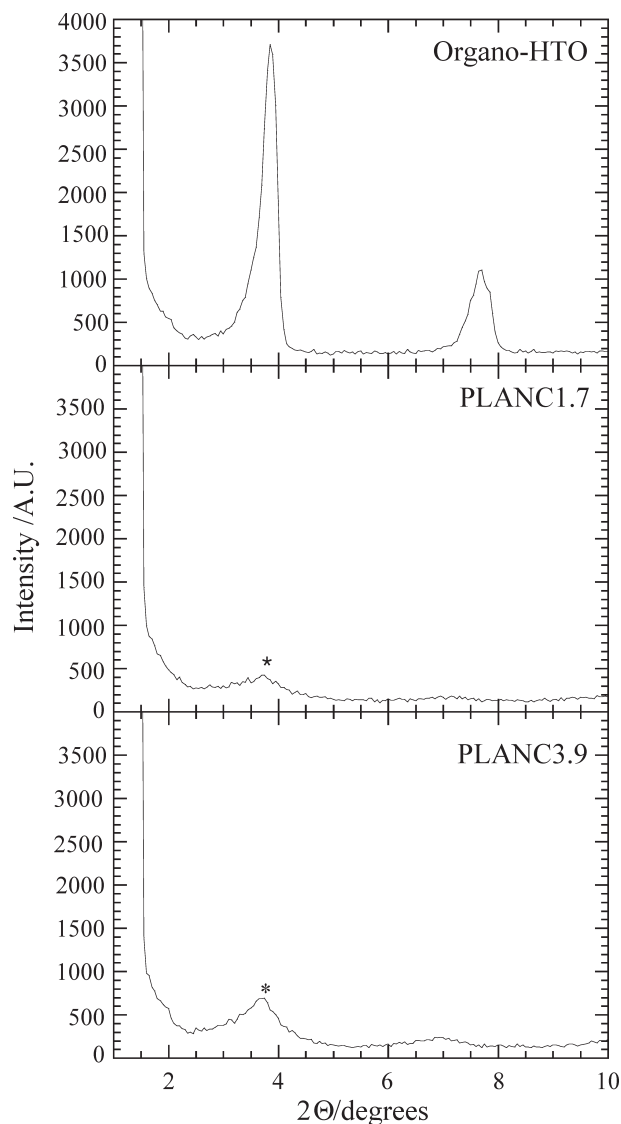


Figure 2. WAXD patterns of OHTO and PLANCs. The asterisks indicate the (001) peak for OHTO dispersed in a PLA matrix.

Table 2. Form factors of nanocomposites obtained from WAXD patterns and TEM images.

Nanocomposite	WAXD			TEM		
	$d(001)$	$D^a)$	$D/d(001)$	$L_{Ti}$	$\xi_{Ti}$	$L_{Ti}/D$
	nm	nm		nm	nm	
PLANC1.7	2.4	11	4.6	$73 \pm 8$	$38 \pm 5$	6–7
PLANC3.9	2.4	14.5	6	$140 \pm 11$	$36 \pm 3$	9–10

<sup>a)</sup> Calculated from the Scherrer equation.<sup>[5]</sup>

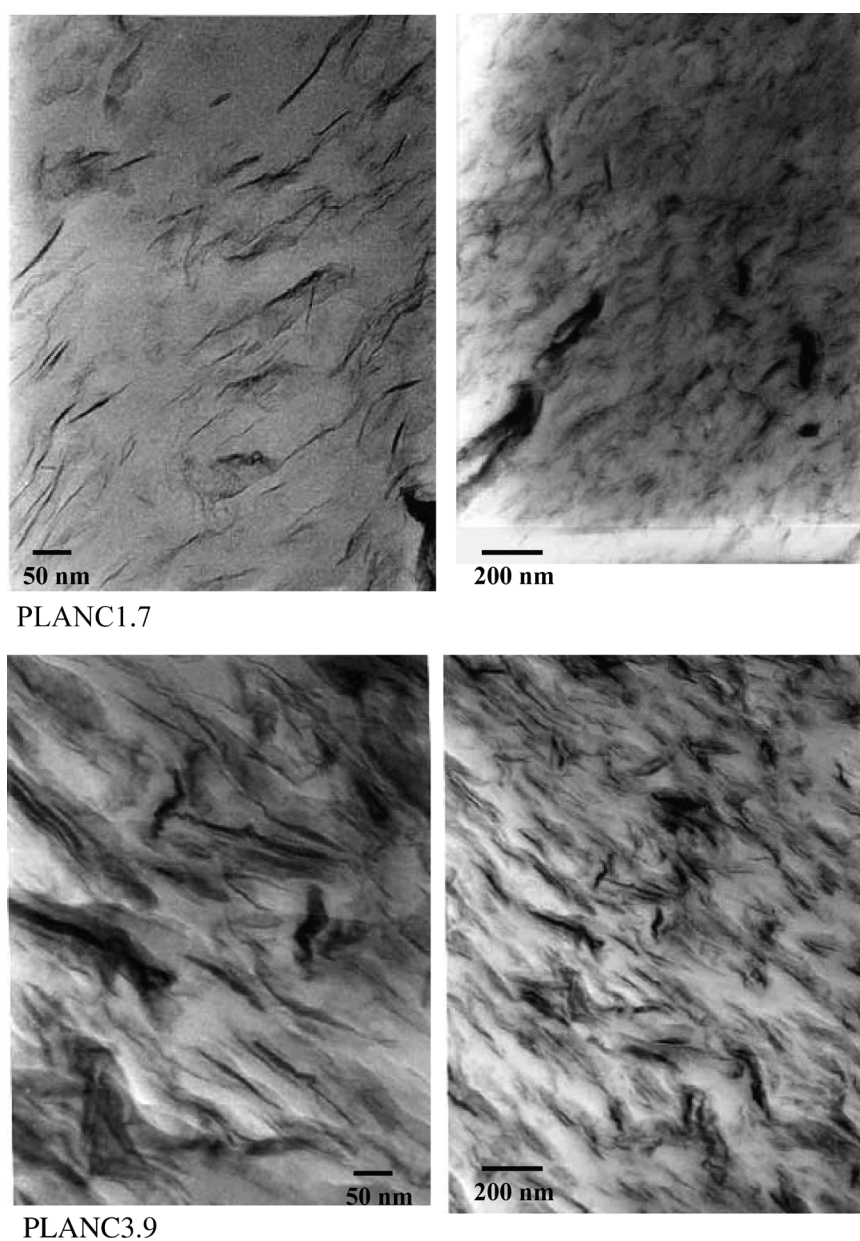


Figure 3. Bright field TEM images observed of crystallized PLANCs pellets.

shown respectively in Figure 2, in which dark entities are the cross section of intercalated OHTO layers.<sup>a</sup> Figure 3 shows both a larger view, showing the dispersion of the titanate layers within the PLA matrix, and a higher magnification, permitting the observation of discrete titanate layers.

The TEM images of PLANCs show fine and almost uniform distribution of titanate particles in the PLA matrix where the titanate particles in both exhibit perpendicular alignment to the sample surface. From the TEM images, it becomes clear that there are intercalated and disordered stacks of titanate layers coexisting in the nanocomposite structure. The intercalated structures are characterized by a parallel stacking that gives rise to the WAXD reflection of PLANC3.9 in Figure 2, whereas the disordered layer formations have no periodic stacking and thus remain WAXD silent. In the case of PLANC3.9, there is a large anisotropy of the stacked titanate layers. The size of some of the stacked-titanate layers appears to reach about 200 nm in lengths. However, we cannot estimate the thickness precisely from the TEM images.

In Table 2, the form factors obtained from WAXD analyses and TEM observations, that is, average length ( $L_{Ti}$ ) and thickness ( $D \equiv d_{Ti}$ ) of the dispersed intercalated titanate layers, and the correlation length ( $\xi_{Ti}$ ) between them, are summarized.<sup>[3]</sup> On the basis of WAXD analyses and TEM observations, we can conclude that PLANCs prepared using OHTO clearly form ordered intercalated nanocomposites with flocculated structure in the case of PLANC3.9, and that coherent order of the titanate layers gradually increases with increasing OHTO content.

In Table 3, we report the flexural modulus and strength of neat PLA and PLANCs measured at 25 °C. There is a significant increase of 38% in the flexural modulus for PLANC1.7 compared with that of neat PLA, and about a 50% increment of modulus in the case of PLANC3.9. On the other hand, flexural strength remarkably decreases with PLANC1.7 and further decreases with PLANC3.9 with increasing OHTO content. This behavior may be caused by the high OHTO content leading to a brittleness of the PLANCs as revealed by their distortion value.

Table 3. Tensile and flexural properties of neat PLA and the nanocomposites.

Samples	Modulus	Strength	Distortion
	GPa	MPa	%
PLA	3.4	108	4.8
PLANC1.7	4.7	86	1.9
PLANC3.9	5	57	1.1

<sup>a</sup> Since the titanate layers are comprised of heavier elements (K, Ti, O) than the interlayer and surrounding matrix (C, H, N, and so on), they appear darker in bright field images.

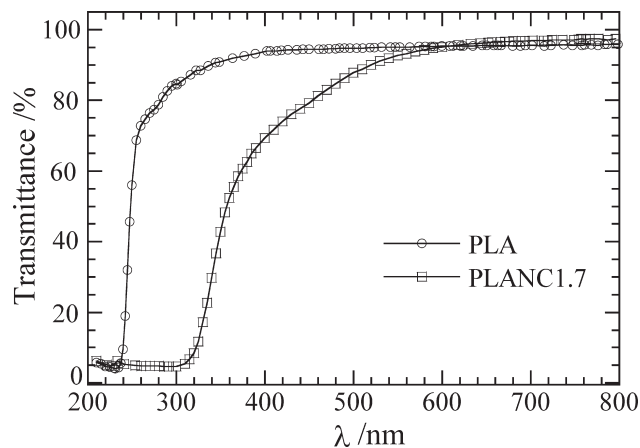


Figure 4. UV/vis transmission spectra of neat PLA and PLANC1.7.

Another interesting aspect of this research is the enhancement of degradability of neat PLA after nanocomposite preparation with OHTO. This may be possible because one of the features of this material is photocatalytic reactivity, in a way similar to titania ( $TiO_2$ ). The photocatalytic reactions of anatase- $TiO_2$ , such as evolution of hydrogen gas from water or oxidative degradation of organic compounds, have attracted intense research interest because of their possible application to the conversion of solar energy into chemical energy.<sup>[7]</sup> Although there are a considerable number of reports concerning the enzymatic and thermal degradation of PLA<sup>[8]</sup> and various PLA blends, there is no data about the photodegradation of PLA and its composites.

Figure 4 shows the UV/vis transmission spectra of pure PLA and PLANC1.7. The spectra show that the visible region ( $> \sim 400$  nm) is changed with increasing absorbency by the presence of titanate layers compared with neat PLA. For UV wavelengths, there is strong absorption up to 320 nm, resulting in 0% transmittance. This significant change in the spectra may indicate the occurrence of photodegradation of the PLA matrix. To confirm this, we conducted some very preliminary experiments on the photodegradation of PLANCs using a sunshine weathermeter at 60 °C. After 300 h, there was no change in the nature of sample surfaces of neat PLA, however, the surface color of the nanocomposite samples became yellow and/or light brown. Table 4 shows the GPC measurement of recovered

Table 4. GPC results of sample recovered from weathermeter after 300 h.

Samples	$\bar{M}_w \times 10^{-3}$	$\bar{M}_w/\bar{M}_n$	$\bar{M}_w/\bar{M}_w^a$
	$g \cdot mol^{-1}$		
PLA	198	1.53	0.94
PLANC1.7	93.7	1.89	0.68
PLANC3.9	86.3	1.86	0.76

<sup>a</sup>  $\bar{M}_w^o$  is the molecular weight before test.

samples from the test. The drop in  $\overline{M}_w$  accompanied with broadening of  $\overline{M}_w/\overline{M}_n$  indicates that the enhancement of degradation of PLA in the OHTO-filled system has occurred. At this moment, we are not able to propose the real mechanism of photodegradation of PLANCs.

## Conclusion

We have successfully prepared novel PLA nanocomposites (PLANC)s using organically modified layered titanate as a new nanofiller. PLANCs exhibit a significant improvement in practical material properties with a simultaneous improvement in degradability under sunshine.

- [1] M. Okamoto, "Polymer/Clay Nanocomposites", *Encyclopedia of Nanoscience and Nanotechnology*, H. S. Nalwa, Ed., ASP, California 2004, Vol. 8, pp. 791–843.
- [2] S. S. Ray, K. Yamada, M. Okamoto, A. Ogami, K. Ueda, *Chem. Mater.* **2003**, *15*, 1456.
- [3] S. S. Ray, K. Yamada, M. Okamoto, A. Ogami, K. Ueda, *Polymer* **2003**, *44*, 6633.
- [4] T. Sasaki, F. Kooli, M. Iida, Y. Michiue, S. Takenouchi, Y. Yajima, F. Izumi, B. C. Chakoumakos, M. Watanabe, *Chem. Mater.* **1998**, *10*, 4123.
- [5] V. A. Drits, C. Tchoubar, "X-Ray Diffraction by Disordered Lamellar Structures", Springer, New York 1990, p. 21.
- [6] R. E. Klimentidis, I. D. R. Mackinnon, *Clays Clay Miner.* **1986**, *34*, 155.
- [7] A. Fujishima, K. Honda, *Nature* **1972**, *37*, 238.
- [8] M. S. Reeve, S. P. McCarthy, M. J. Downey, R. A. Gross, *Macromolecules* **1994**, *27*, 825, and references cited therein.